(2) For example: (a) Heatley, F. *Progress in NMR Spectroscopy* Pergamon: London, 1979; Vol. 13, p 47. Connolly, J. J.; Gordon, E.; Jones, A. A. *Macromolecules* **1984**, *17*, 722.
(3) For example: Patterson, G. D.; Stevens, J. R.; Alms, G. R.; Lindsey, C. P. *Macromolecules* **1979**, *12*, 661. Fytas, G.; Ngai, K. L. *Macromolecules* **1988**, *21*, 804.
(4) Bullock, A. T.; Cameron, G. G.; Smith, P. M. *J. Chem. Soc., Faraday Trans. 2* **1974**, *70*, 1202.
(5) Hyde, P. D.; Waldow, D. A.; Ediger, M. D.; Kitano, T.; Ito, K. *Macromolecules* **1986**, *19*, 2533.
(6) Waldow, D. A.; Hyde, P. D.; Ediger, M. D.; Kitano, T.; Ito, K. *Photophysics of Polymers*; ACS Symposium Series 358; American Chemical Society: Washington, DC, 1987; p 68.
(7) Viovy, J. L.; Monnerie, L.; Brochon, J. C. *Macromolecules* **1983**, *16*, 1845.
(8) Viovy, J. L.; Monnerie, L. *Polymer* **1986**, *27*, 181.
(9) Valeur, B.; Kasparyan, N.; Monnerie, L. *26th Int. Symp. Macromol. Mainz* **1979**, *2*, 989.
(10) Ricka, J.; Amlser, K.; Binkert, Th. *Biopolymers* **1983**, *22*, 1301.
(11) Phillips, D. *Polymer Photophysics: Luminescence, Energy Migration, and Molecular Motion in Synthetic Polymers*; Chapman and Hall: London, 1985.
(12) Sasaki, T.; Yamamoto, M.; Nishijima, Y. *Makromol. Chem. Rapid Commun.* **1986**, *7*, 345.
(13) Sasaki, T.; Yamamoto, M.; Nishijima, Y. *Macromolecules* **1988**, *21*, 610.
(14) Kivelson, D. In *Rotational Dynamics of Small and Macromolecules*; Dorfmuller, Th., Pecora, R., Eds.; Springer-Verlag: Berlin, 1987; p 1.
(15) *International Critical Tables*; McGraw-Hill: New York, 1930; Vol. 7, p 211.
(16) (a) Wagner, H. L.; Flory, P. J. *J. Chem. Phys.* **1952**, *74*, 195. (b) Poddubnyi, I. Ya., Ehrenburg, E. G. *J. Polym. Sci.* **1962**, *57*, 545. (c) Hadjichristidis, N.; Roovers, J. E. L. *J. Polym. Sci.* **1974**, *12*, 2521.
(17) Hall, C. K.; Helfand, E. *J. Chem. Phys.* **1982**, *77*, 3275.
(18) Kubo, R.; Toda, M.; Hashitsume, H. *Statistical Physics II: Nonequilibrium statistical Mechanics*; Springer-Verlag: Berlin, 1985; p 42.
(19) *Polymer Handbook*, 2nd ed.; Brandrup, J., Immergut, E. H., Eds.; Wiley: New York, 1975.
(20) Bauer, D. R.; Brauman, J. I.; Pecora, R. *Macromolecules* **1975**, *8*, 443.
(21) (a) Riseman, J.; Kirkwood, J. G. *J. Chem. Phys.* **1949**, *17*, 442. (b) Zimm, B. H. *J. Chem. Phys.* **1956**, *24*, 269. (c) Isihara, A. *J. Chem. Phys.* **1967**, *47*, 3821.
(22) Flory, P. J. *Statistical Mechanics of Chain Molecules*; Wiley Interscience: New York, 1969; p 52.
(23) Waldow, D. A.; Johnson, B. S.; Babiarz, C. L.; Ediger, M. D.; Kitano, T.; Ito, K. *Polym. Commun.* **1988**, *29*, 296.
(24) The self-avoiding random walk utilized six possible step directions of equal probability. If any given step visited a site previously visited, the walk was thrown out and restarted. For self-avoiding walks greater than 48 segments, the enrichment method of Wall and Erpenbeck was utilized (Wall, F. T.; Erpenbeck, J. J. *J. Chem. Phys.* **1959**, *30*(3), 634).
(25) For a general discussion of the use of random walk models for good and Θ solvent conditions, see: de Gennes, P.-G. *Scaling Concepts in Polymer Physics*; Cornell University Press: Ithaca, NY, 1979; p 29.
(26) Schaefer, D. W.; Han, C. C. *Dynamic Light Scattering*; Pecora, R., Ed.; Plenum: New York, 1985; p 181.
(27) Heatley, F.; Begum, G. *Polymer* **1976**, *17*, 399.
(28) Weber, T. A.; Helfand, E. *J. Phys. Chem.* **1983**, *87*, 2881.

# Dynamics of Gel Electrophoresis

**Edward O. Shaffer II and Monica Olvera de la Cruz***

*Department of Materials Science and Engineering, Northwestern University, Evanston, Illinois 60208.* *Received May 19, 1988; Revised Manuscript Received August 18, 1988*

ABSTRACT: An off-lattice computer simulation based on the Langevin equation of motion is used to study gel electrophoresis. The simulated chain dynamics are dramatically different from the dynamics predicted by tube-reptation theories. The mobility of different length chains is traced, showing the loss of length dependence as the field is increased. The dynamics of the chain in the field-independent mobility regime are illustrated.

## Introduction

Gel electrophoresis has great importance in modern molecular biology as a method for separating proteins and nucleic acids, in particular DNA. In its simplest form, the technique consists of applying a constant electric field to a gel that contains the molecules of interest. In the limit of small electric fields, the mobility of linear polymer chains is inversely dependent on length. After a period of time, the chains of different sizes separate physically in the gel. Unfortunately, for higher electric fields, the inverse length dependence of the mobility is strongly reduced. This loss of length-dependent mobility occurs at smaller fields for larger chains. Consequently, the technique is unable to separate very long chains.[1] In an effort to optimize the separation process, more sophisticated approaches have been developed.[2,3] Despite the importance of gel electrophoresis, the dynamics of this process are still not fully understood. Experimental developments have relied solely on empirical observations.

In order to understand the dynamics of gel electrophoresis and why the mobility loses its inverse length dependence, we have developed an off-lattice computer program of the process. The results of the simulation illustrate a diffusional process not explained by the existing tube-reptation theories of gel electrophoresis.[4,5]

de Gennes[6a] introduced the reptation model to explain the dynamics of long linear chains in a gel with no applied forces. The diffusion of an ideal chain of $N$ units of length $b$ is restricted by the gel. The reptation model accounts for this restriction by confining the polymer to diffuse along the random path of a tube. The tube's diameter is the average distance between network junction points, $a$. For distances less than the tube diameter, $a$, the polymer moves freely. For larger distances, the chain is constrained to diffuse along the tube path. The tube consists of $N'$ segments of length $a$ where $N' = Nb^2/a^2$. The contour length of the tube, $L$, is given by

$$L = N'a \tag{1}$$

In tube-reptation theories, for diffusion larger than the tube diameter, all the lateral motion perpendicular to the tube is explicitly ignored. Only the end tube segments are free to move. As a result, the path of the chain is determined by the end tube segments.

Current gel electrophoretic theories are based on the tube-reptation concept constraining the chain to move

0024-9297/89/2222-1351$01.50/0 

along a tube path.[4,5] Tube theories of gel electrophoresis assume that the steady-state chain configuration is known even though it is not obtainable by statistical mechanics.[6b] They postulate that fluctuations in the tube contour length, $L$, are negligible and are uncorrelated to the mean square end-to-end distance of the chain in the field direction, $h_x^2$. In the presence of an electric field, tube-reptation theories posit that the leading tube segment is biased in the field direction. This bias gives rise to an average orientation proportional to the field strength. The orientation is assumed to accumulate in proportion to the number of tube segments, $N'$. The mobility (defined by the velocity of the chain's center of mass in the field direction, $V_{cm}^x$, divided by the applied field, $E$) is given by tube-reptation theories[4] as

$$\mu = \frac{Q}{\xi_c}\langle h_x^2/L^2\rangle \tag{2}$$

where $Q$ is the total charge along the chain and $\xi_c$ is the translational coefficient of friction of the chain. With the assumptions described above and for a periodic system of obstacles with spacing $a$, the tube-reptation mobility[4b] for small electric fields reduces to[7]

$$\mu = \frac{Q}{3\xi_c}\left(1/N + \frac{1}{3}\left(\frac{E'a}{2}\right)^2\right) \tag{3}$$

where $E' = aq/2kT$ is a dimensionless reduced electric field, $q$ is the charge per tube segment of length $a$, and $kT$ is the thermal energy.

Equation 3 recovers the expected change in mobility for increasing fields. If the predictions of (3) are compared to experimental results,[1,8] the model appears to fit qualitatively in the limit of small fields. Tube-reptation theories predict the mobility to increase with increasing field until, for large enough fields, the chain is completely oriented.[5] However, experiments show that saturation occurs at lower fields than predicted by tube-reptation theories.[8] Also, in tube-reptation theories the saturated chain's mobility, for tube segments of constant size, reduces to the mobility of a free chain:[5]

$$\mu = Q/\xi_c \tag{4}$$

However, the experimental results[8] show that the mobility plateaus at a much lower mobility than predicted by (4). Corrections to tube-reptation theories, like introducing a distribution of tube segments,[4] do not account for the discrepancies with experimental results. Also, other experiments[9] where the applied field is periodically inverted and/or rotated yield mobilities that tube theories cannot account for.

The main assumption of tube-reptation theories is that diffusive fluctuations of internal segments through the entanglements is nearly impossible due to the entropic penalty associated with this type of motion. As a result, the diffusion in tube-reptation theories is governed by the dynamics of the end tube segments. However, as the field strength is increased, there is an added tensile force acting along the internal segments, causing the chain to fluctuate through the entanglements. In the limit of zero field, this tension disappears and the chain continues to diffuse via Brownian motion in the tube. As the field is increased, the fluctuations through the tube increase. The tube-reptation theory is no longer able to describe the dynamics of the chain.

A recent study of gel electrophoresis by Deutsch[10a] illustrates the effects of these fluctuations through the entanglements. He finds that at large fields, $Elq/kT > 1$ where $l$ is the persistence length of the chain, the dynamics deviate dramatically from tube theories. Deutsch directly simulates the motion of the chain by solving numerically the chain's Langevin equation of motion. He showed that the field causes the chain to slip around the entanglements in the direction of the longer side of the chain. As the longer side of the chain grows, a tension develops in the chain, causing it to extend. The chain does not remain fully extended. The front segments of the chain have lower mobility since they encounter an additional friction due to collisions with the entanglements. The chain consequently falls on itself, forming a rather dense ball in the fron of the chain. Eventually, the whole chain is eaten up by the ball. The entanglements rehood the balled-up chain. The process then repeats itself with the chain continually unhooking and hooking.

In this paper, we concentrate in the regime where these fluctuation effects are increasingly noticeable. For very small fields, we recover the length-dependent mobilities predicted from tube theories. For larger fields, we find the mobility increasing faster than predicted by tube theories. Also, the mobility plateaus to values less than the predicted mobility of a free chain. The dynamics are similar to those described by Deutsch.

## Computer Simulation

The computer simulation is a two-dimensional off-lattice model. The polymer chain in the gel is assumed to be at its Θ temperature; hence, the polymer statistics are Gaussian.[11] For simplicity, hydrodynamic effects are ignored. Consequently, the chain can be modeled as a Rouse chain, i.e., as a system of beads connected by entropic springs. Each Rouse spring consists of four random-walk persistence lengths, $b$, such that the average end-to-end distance of the spring is zero. The chain is comprised of $N$ beads connected by $N - 1$ springs. Modeling the chain as a Rouse chain is appropriate for the field strengths and gel spacings used in this simulation since monomer–gel interactions are negligible. For higher fields and/or tighter gels, the specific monomer configuration is important and the monomer–gel interactions must be accounted for, making the Rouse model inapplicable.[10b,12] The gel is represented as a system of fixed entanglement points of regular spacing $a$.

In the simulation, the bead-spring dynamics are determined by the Langevin equation of motion. The Langevin equation includes the effect of thermal forces, viscous drag forces, entropic spring forces, and applied field forces. In the Langevin approach, inertial effects are ignored. The Langevin equation for the position of the $i$th bead, when no gel is present, is written as

$$\partial r_i(t)/\partial t = \eta_i + F_{spr}/\xi_b + F_{elc}/\xi_b \tag{5}$$

where $r_i(t)$ is the position of the $i$th bead in space at time $t$ and $\xi_b$ is the translational friction coefficient of the bead. $\eta_i$ is the thermal force due to the high-frequency fluctuations of the beads in the medium and is characterized by

$$\langle \eta_i(t)\rangle = 0$$
$$\langle \eta_i(t)\eta_j(t')\rangle = 2D_b\delta(t - t')\delta(i - j) \tag{6}$$

$D_b$ is the diffusion coefficient for the bead given by the Einstein relation

$$D_b = kT/\xi_b \tag{7}$$

The entropic spring forces, $F_{spr}$, are Hookean and are given by

$$F_{spr} = 2kT\{r_{i+1}(t) + r_{i-1}(t) - 2r_i(t)\} \tag{8}$$

The electric force is defined as the electric field, $E$, times

the charge, $q$. The simulation electric force, $E_s$, is a dimensionless force defined as

$$E_s = Eq_s l_s/kT \tag{9a}$$

where $q_s$ is the charge per spring[13] and $l_s$ is referred to as the spring length. $l_s$ is the square root of the mean square end-to-end distance of the springs in the absence of an electric field. As there are four persistence lengths, $b$, per spring,

$$l_s = 2b \tag{9b}$$

According to the Langevin equation (5), the position of the $i$th bead at a time $t + \tau$ is

$$r_i(t + \tau) = r_i(t) + \eta_i + [D_b E_s + 2D_b\{r_{i+1}(t) + r_{i-1}(t) - 2r_i(t)\}]\tau \tag{10}$$

In the simulation, the gel is represented by a square lattice of fixed entanglement points. The spacing between entanglement points, $a$, is equal to four persistence lengths, $a = 4b$.

The dynamics are introduced by iteration. At each computer iteration, a random permutation from 1 to $N$ is generated. The beads are moved in order of the permutation. Time is advanced by $\tau$ after all beads have moved. At each iteration, the bead is moved to a temporary position, $r_i'$, according to (10). The algorithm tests to see if any gel point is crossed by the springs attached to the bead during the move from $r_i(t)$ to $r_i'$. If a gel point is crossed, then the move is rejected and $r_i(t + \tau)$ is set equal to $r_i(t)$. If no gel point is crossed, then the move is accepted.

$\tau$ is chosen to be very small to simulate continuous drift. The simulation results rescale with $\tau$ preserving continuity.[12] The simulation also recovers the predicted reptation results for zero field.[12]

The dynamical quantities calculated are the center of mass motion and the radius of gyration as a function of time. The time units are computer time, $t_c$ (the number of iterations), multiplied by $\tau$ and the diffusion coefficient of the bead, $D_b$, divided by the square of the spring length, $l_s^2$. In the simulation, $l_s$, given by (9b), is set equal to one. Therefore, one unit length in the simulation equals two persistence lengths.

## Results and Discussion

We ran the simulation for three different length chains, $N = 40, 60, 80$, for field strengths from $E_s = 0.010$ to 0.150. All simulations were ran for cage spacings equal to four persistence lengths, $D_b = 1.0$, and $\tau = 0.05$. The simulation was run on the CRAY X-MP at the National Center for Supercomputing Applications, Champaign, IL. Unfortunately, due to computer time limitations, only 10 runs were repeated and averaged. In order to obtain better chain statistics, more repeats are needed.

The center of mass motion in the field direction is plotted in Figure 1 for $N = 60$. The plot shows the expected linear diffusion of the center of mass. The mobility is calculated by dividing the slopes of these curves by the respective field strength. The mobility as a function of field strength is plotted in Figure 2 for the three different chains. Qualitatively, the mobility data agree with experimental results found by Hervert and Bean.[8] For small fields, the mobility recovers the inverse length dependence predicted by tube theories. However, the mobility increases more quickly than predicted by tube-reptation theories. Also, the mobility plateaus to a value less than the mobility of a free chains ($\mu = 1$ in our simulation), as (4) based on tube assumptions predicts.

The simulation breaks down for fields at which the tensile force acting on the beads dominates the spring

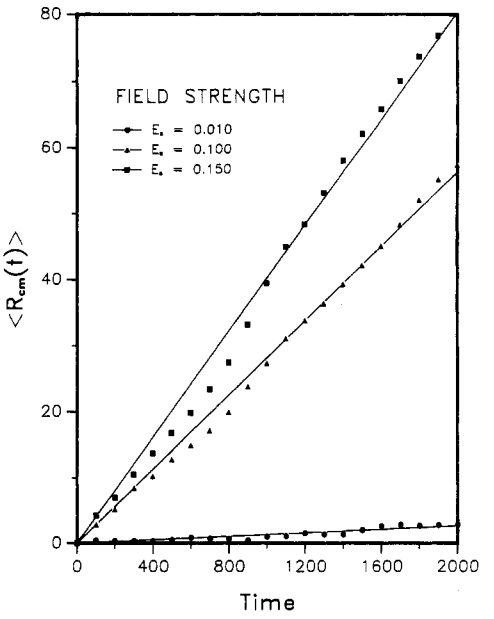


**Figure 1.** Center of mass in the field direction, $\langle R_{cm}(t)\rangle$, versus time for $N = 60$.

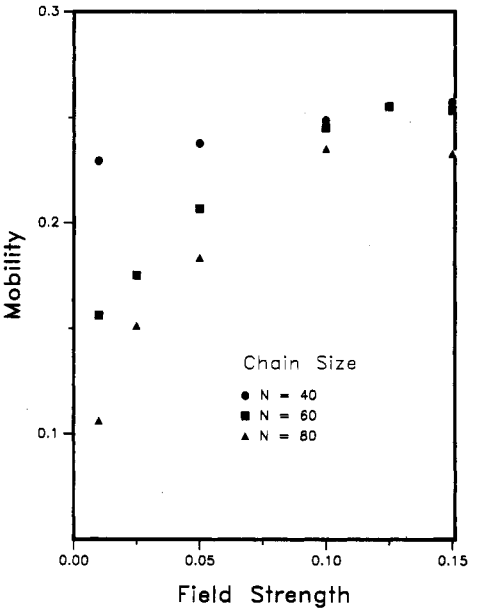


**Figure 2.** Mobility versus field strength, $E_s$, for three different length chains. The plots show the loss of length dependence for increasing fields.

forces. In such a case, the spring is effectively pinned by the entanglement and stretches because the model does not allow the springs to rotate around the entanglements. As a result, the chain's center of mass becomes trapped. The decreasing trend in the mobility at $E_s = 0.150$ is a result of this local pinning introduced by the model. In order to study the gel electrophoresis for higher fields, a simulation that allows for rotation is needed. For the field strengths of interest in this simulation, the springs are able to recover Gaussian statistics and the center of mass continues to diffuse linearly with time.

Figure 3 illustrates the dynamics of a chain at $E_s = 0.150$. The dynamics deviate greatly from those predicted by tube-reptation theories of gel electrophoresis. Figure 3a is the initial configuration of a random chain. By time equal to 100, Figure 3b, the chain ends have started diffusing in the field direction. But at time equal to 200, Figure 3c, we see the internal segments of the chain starting to fluctuate through the entanglements. As the

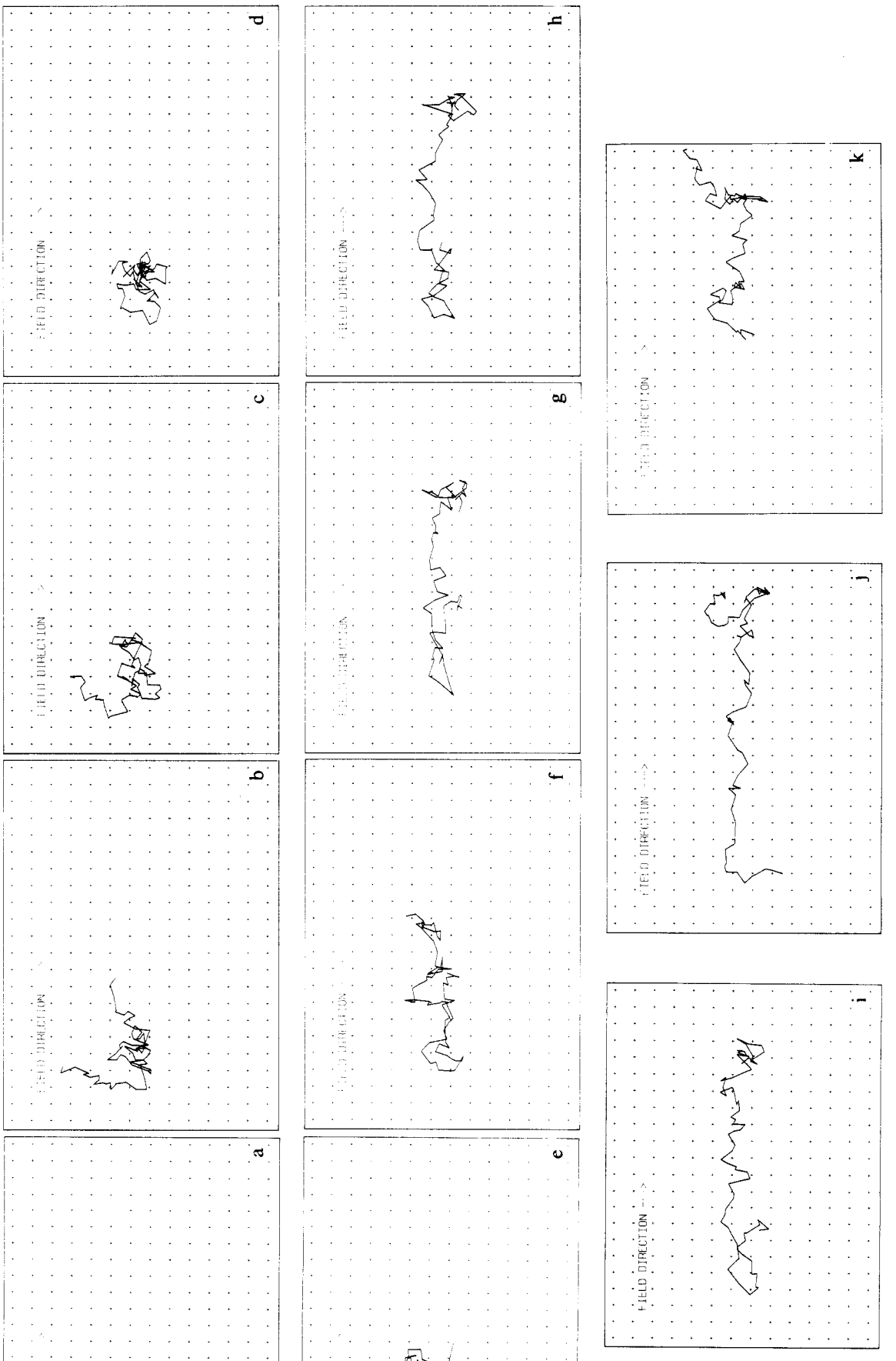


**Figure 3.** Position of a chain, $N = 80$, in a gel for $E_s = 0.150$ at different times: (a) $t = 0$, (b) $t = 100$, (c) $t = 200$, (d) $t = 300$, (e) $t = 400$, (f) $t = 500$, (g) $t = 600$, (h) $t = 700$, (i) $t = 800$, (j) $= 900$, (k) $t = 1000$. The sequence illustrates the dynamics of a chain in the field-independent regime.

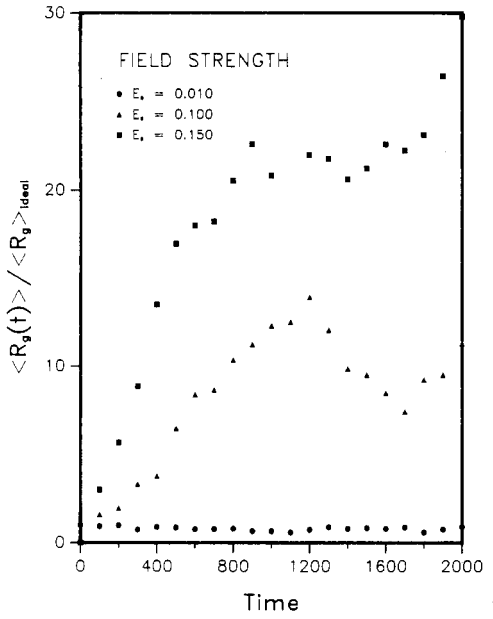


**Figure 4.** Radius of gyration, $\langle R_g(t) \rangle$, divided by the ideal radius of gyration for a chain $N = 80$ for different field strengths.

chain slips past the entanglements, it forms a dense ball, Figure 3d. Notice that the ends have collapsed into the ball as well. Parts a–d of Figure 3 illustrate quite well that the ends are no longer determining the dynamics of the chain.

For time equal to 400, Figure 3e, we note that the chain is still hooked about one entanglement. This hook results in the chain unraveling in the direction of the field, forming a U-shape about the entanglement, parts e and f of Figure 3. As the chain elongates, a tension builds in the chain which results in the long end of the chain growing at the expense of the short end, parts f–i of Figure 3. By time equal to 900, the chain is free of the entanglement, Figure 3j.

Note that as the chain unravels the leading chain segments begin to ball up again, Figure 3g. This leading ball is due to the extra friction experienced by the leading segments as they collide with additional entanglements. Since the leading segments experience more friction, the mobility of the leading segments is lower, allowing the rest of the chain to catch up. However, before the chain can ball up into a dense ball, as in Figure 3d, the leading segments begin to slide around the entanglements again. For very high fields, we would expect the chain to be able to catch up with itself, resulting in the formation of a very dense ball.

The dynamics of the chain unraveling and balling up is evident in the oscillations of the radius of gyration. Figure 4 plots the radius of gyration versus time for $N = 80$. For higher fields, the oscillations become increasingly more pronounced. For $E_s$ equal to 0.010, where field-dependent mobilities are recovered, the chain remains Gaussianly distributed. Also, for smaller chains, the oscillations have lower amplitude and shorter periodicity.[12] We speculate that these varied statistics of different length chains can explain the mobility results of field inversion/rotation techniques.[9]

The dynamics illustrated in Figure 3 point out that the chain does not follow the tube path but fluctuates through the entanglements.[14] As a result, the mobility loses its inverse dependence on chain length at fields lower than predicted by tube-reptation theories. The entanglements introduce an additional friction along the chain, resulting in the mobility plateauing to a value less than the mobility of a free chain.

## Conclusion

The simulation illustrates the dynamics of gel electrophoresis in the regime of length-independent mobility. The dynamics deviate greatly from the dynamics predicted by current tube-reptation theories. In this regime, the chain slides past the entanglements, resulting in the length-independent mobility. The additional friction introduced by this motion causes the mobility to plateau at values less than the mobility of a free chain.

**Acknowledgment.** Acknowledgment is made to the donors of the Petroleum Research Fund, administered by the American Chemical Society, for partial support of this research. We also thank the National Science Foundation for financial support through the Materials Research Center at Northwestern University by Grant DMR 8520280. Finally, we thank J. Deutsch for sending us his unpublished results[10a] while we were completing this work.[15]

## References and Notes

(1) McDonnel, M. W.; Simon, M. N.; Studier, F. W. *J. Mol. Biol.* **1977**, *110*, 119.
(2) Stellwagen, N. C. *J. Biomol.* **1985**, *3*, 299.
(3) Schwartz, D. C.; Cantor, D. R. *Cell* **1984**, *37*, 67.
(4) (a) Lumpkin, O. J.; Zimm, B. H. *Biopolymers* **1982**, *21*, 2315. (b) Lumpkin, O. J.; DeJardin, P.; Zimm, B. H. *Biopolymers* **1986**, *25*, 431.
(5) Slater, G. W.; Noolandi, J. (a) *Phys. Rev. Lett.* **1985**, *55*, 1579; (b) *Biopolymers* **1986**, *25*, 431.
(6) (a) de Gennes, P.-G. *J. Chem. Phys.* **1971**, *55*, 572. (b) In the reptation model,[6a] the knowledge of the chain statistics allows us to construct a ficticious "tube" whose statistics have to follow the chain configuration in the gel. In the presence of an electric field, however, the steady-state configuration of the chain is not obtainable by statistical mechanics. The tube-reptation theories of gel electrophoresis have to postulate the "tube" statistics and the chain configuration.
(7) In this paper, we will only analyze the diffusion of long chains, $bN \gg a$. For short (rigid) chains, the mobility varies as $\ln N$,[1] in agreement with the theoretical results for rod diffusing in a matrix of obstacles, studied by: de Gennes, P.-G. *C. R. Acad. Sci. Paris* **1982**, *294*, 827.
(8) Hervert, H.; Bean, C. P. *Biopolymers* **1987**, *26*, 727.
(9) Carle, G. F.; Frank, M.; Olson, M. V. *Science* **1986**, *232*, 65.
(10) Deutsch, J. M. (a) *Science* **1988**, *13*, 922; (b) *Phys. Rev. Lett.* **1987**, *59*, 1255.
(11) We believe that adding excluded volume interactions will not change qualitatively the results found in this paper. The effects of the excluded volume interaction will be investigated in future simulations.
(12) Shaffer, E. O. Dynamics of Gel Electrophoresis. Masters of Science Thesis, Northwestern University, Evanston, IL, 1988.
(13) $q_s$ is referred to as the electrophoretic charge. In DNA, $q_s$ is approximately half the actual DNA phosphate groups charge due to the adsorption of counterions. Screening effects in the DNA electrophoretic charge in monovalent salt solutions are discussed by: Schollman, J. A.; Stigter, D. *Biopolymers* **1977**, *16*, 1415.
(14) Similar effects in the chain configuration during pulsed field DNA gel electrophoresis were found by: Holzwarth, G.; McKee, C. B.; Steiger, S.; Crater, G. *Nucleic Acids Res.* **1987**, *15*, 10031.
(15) J. M. Deutsch's approach[10a] differs from ours in that he does not use the bead and spring model. In his analysis, the tension along the chain at time $t$ is calculated, and the chain is moved according to this calculated tension. In the next step, $t + \tau$, the process is repeated.